# Viability of using near infrared PbS quantum dots as active materials in luminescent solar concentrators

G. V. Shcherbatyuk,[1] R. H. Inman,[1] C. Wang,[2] R. Winston,[1,2] and S. Ghosh[1,a)]
[1]*School of Natural Sciences, University of California, Merced, California 95343, USA*
[2]*School of Engineering, University of California, Merced, California 95343, USA*

(Received 16 February 2010; accepted 13 April 2010; published online 11 May 2010)

The performance of chemically synthesized lead sulfide (PbS) quantum dots (QDs) in planar, nontracking luminescent solar concentrators (LSCs) is evaluated using spectroscopic and photovoltaic techniques. Spatially resolved measurements are used to investigate and analyze the role of reduced self-absorption on the LSC efficiency. From comparative measurements of samples with Rhodamine B and CdSe/ZnS QDs it is established that PbS LSCs generate nearly twice the photocurrent in silicon cells than the other materials, achieving an integrated optical efficiency of 12.6%. This is attributed primarily to the broadband absorption of PbS which allows optimum harvesting of the solar spectrum. © *2010 American Institute of Physics*. [doi:10.1063/1.3422485]

A luminescent solar concentrator (LSC)[1,2] absorbs a portion of the incident solar radiation and re-emits it at a longer wavelength. Confined to the plane of the LSC by total internal reflection, this down-shifted radiation is concentrated onto PV cells attached at edges of the plate [Fig. 1(a)]. While the photocurrent of an LSC is lower than an equivalently sized PV panel because of loss mechanism introduced by the collector, the photocurrent generated by the edge cells may increase relative to the same cell facing the sun because of the concentration effect at the LSC edges. Additionally, LSCs perform very well under both direct and diffuse lighting conditions.[3,4] This negates the need for any tracking mechanisms, further reducing operating costs for solar powered devices and allowing for applications such as building integrated PVs.

The achievable efficiency in LSCs is dependent on the optical properties of the absorbing fluorescent material and on how well it is spectrally matched with the attached PV cell, and recently, inorganic compounds have emerged as attractive candidates.[5–7] Among these, semiconducting quantum dots (QDs) are particularly suitable, possessing a broad band absorbance, high quantum yield, and size-tunable emission characteristics.[8] All experimental studies to date have been restricted to QDs with absorption and emission bands in the visible region of the electromagnetic spectrum, despite the fact that over 60% of the total solar photon flux occurs at wavelengths greater than 600 nm. Another motivation for designing infrared QD LSCs is that by size selection the QD emission can be positioned to match the band-gap of silicon PV cells. This serves to enhance the external quantum efficiency of silicon cells,[9] and therefore, the power conversion efficiency (PCE) of the device. In this letter, the properties of chemically synthesized 2.2 nm PbS QDs with emission centered in the near infrared region are investigated to gauge their viability as the active material in an LSC coupled to silicon PV cells.

The QD samples are commercially purchased (Evident Technologies) and dispersed in toluene. While a functional LSC requires that the fluorescent material be encapsulated in a solid matrix, that would further alter the optical properties of the QDs, such as induce spectral blueshifts and reduce quantum yields.[10] For our purposes of fundamental studies, liquid solutions are sealed into quartz panels of dimensions $45\times12\times4$ mm$^3$ (optical path length of 2 mm). At the short edge of the panel, a silicon PV cell is attached [Fig. 1(a)] with an active area of $12\times3$ mm$^2$. The absorption spectra are taken with a Perkin Elmer UV-VIS spectrometer, and the emission spectra with a 300 mm Acton spectrometer with a thermoelectrically cooled charged-coupled device (resolution 0.14 nm).

The integrated optical efficiency ($\eta_{opt}$) of an LSC is governed by the absorption efficiency ($\eta_{abs}$), retention losses ($\eta_L$), and quantum yield ($\eta_{QY}$) of the fluorescent material.[7] The QDs ideally need to absorb as high a percentage of the incident solar radiation as possible. Figure 1(b) shows a comparison of the absorption spectra between CdSe/ZnS and PbS QDs. It illustrates the following: first, to have equivalent absorbance, the concentration of the PbS

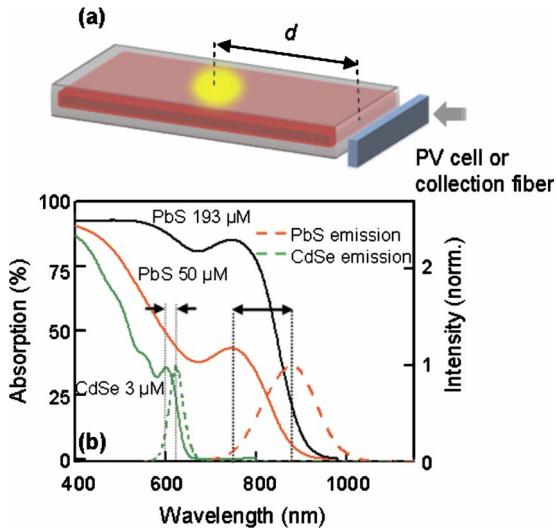


FIG. 1. (Color online) (a) Schematic of the device highlighting the arrangement of PV cell/collection fiber with relation to the excitation beam. (b) Absorption curves in absolute units for CdSe/ZnS and PbS QDs. Overlaid emission curves (dashed) for CdSe/ZnS and PbS QDs with Stoke's shift marked by double headed arrows.

a)Author to whom correspondence should be addressed. Electronic mail: sghosh@ucmerced.edu.

 

solution needs to be higher than that of the CdSe/ZnS QDs. This is understandable as the molar extinction coefficient $\varepsilon = 2 \times 10^4$ L mol$^{-1}$ cm$^{-1}$ for PbS and $3 \times 10^5$ L mol$^{-1}$ cm$^{-1}$ for CdSe/ZnS, and the absorbance $A$ varies as $A = \varepsilon c l$ ($c$ is the concentration and $l$ is the optical path length); second, the spectral range over which the QDs absorb is more extensive for PbS. While CdSe/ZnS absorbs significantly over $<600$ nm, PbS has similar absorbance over $<800$ nm, which means that the PbS QDs will absorb the solar spectrum far more effectively.

As the absorbed radiation is re-emitted there are two main loss mechanisms that affect the number of the photons that are transported to the edges. For a typical polymer or glass matrix with a refractive index ~1.5, about 25% of the emission solid angle is directed through the top surface.[11] However, the fraction of photons lost through this surface is actually much higher due to multiple absorption and emission events. Another significant percentage is lost through "self-absorption"[12] (SA), which is reabsorption of the emitted photons by the emitters. It is also the reason that LSCs cannot use an arbitrarily high concentration of the fluorescent species. Figure 1(b) also plots the emission spectra of the QDs normalized to the first emission peaks. For both materials, the absorption band partially overlaps the emission band and the greater this overlap, the more pronounced the SA. The CdSe/ZnS dots show a very large overlap with a Stoke's shift of 23 nm, and the absorption at the emission peak is about 0.68. In comparison, the absorption and emission curves of PbS show a much larger Stoke's shift of 122 nm, and the absorption falls to 0.24 at the emission peak.[13]

To qualitatively verify the role of SA, spatially resolved spectral measurements are performed. The QD filled quartz panel is mounted on an automated translation stage and coupled to an optical fiber at the short edge in place of the PV cell shown in Fig. 1(a). A collimated beam from a laser tuned to 407 nm (CdSe/ZnS) or 632 nm (PbS) is used to excite a localized spot on the sample. The distance $d$ between the excitation point and the collection fiber at the edge is varied continuously by translating the sample. As $d$ increases and the photons negotiate a longer path length, the probability that an emitted photon will be self-absorbed by a QD goes up. This absorbed photon, if re-emitted, undergoes a redshift which is evident as a net shift in the emission spectrum toward longer wavelengths. The amount of this redshift is a measure of the extent of SA in the sample.[7] Figure 2(a) shows normalized spectra for the 50 $\mu$M solution of PbS at $d=0$, 10, and 20 mm. Regardless of the excitation-collection separation, the emission spectrum appears to have a bimodal distribution with peaks at $\lambda_1 = 896$ nm and $\lambda_2 = 928$ nm, which most likely arises from two fractions of differently sized dots in the ensembles.[14] With increasing $d$, the spectral weight shifts from $\lambda_1$ to $\lambda_2$ as the emission from the smaller dots are increasingly absorbed and re-emitted by the larger ones. Individually the peak at $\lambda_1$ shifts by ~4 nm and the one at $\lambda_2$ by ~2 nm between $d=0$ and 20 mm. CdSe/ZnS QD emission with equivalent absorbance shows a redshift of almost 20 nm by $d=20$ mm. Since the 50 $\mu$M sample shows relatively small SA, the measurement is repeated with a 193 $\mu$M (stock concentration) solution of PbS. This sample shows very high absorption [Fig. 1(b)], and its emission spectrum shows a single peak at 928 nm at $d=0$ [Fig. 2(b)]. The decimation of the previously observed $\lambda_1$ implies that in the 193 $\mu$M solution the luminescence from the smaller dots is quenched. As $d$ is increased, the spectrum redshifts and this shift in the peak of emission from the $d=0$ value is plotted in the inset (solid circles), along with the observed redshift in the 3 $\mu$M CdSe/ZnS solution (open circles). The former saturates around $\Delta\lambda = 20$ nm but the latter keeps increasing up to the limits of the measurement capability.

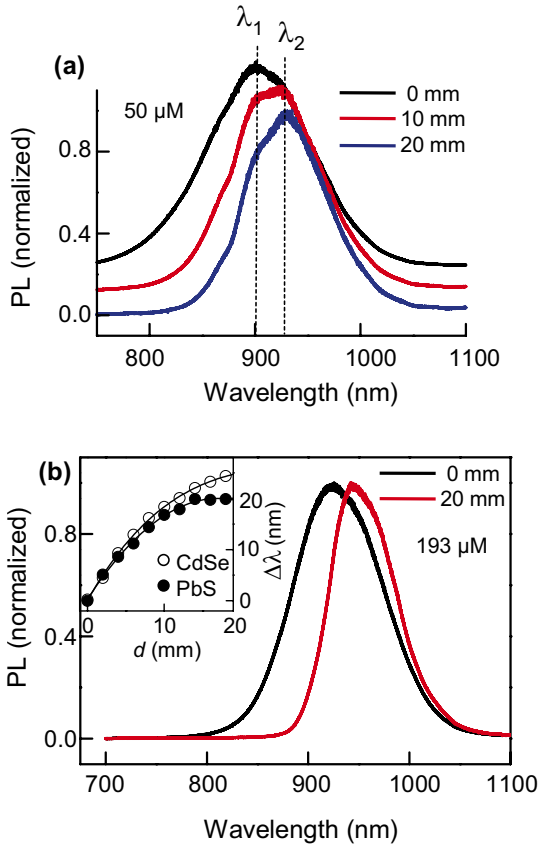


FIG. 2. (Color online) (a) The effect of changing the distance between excitation and collection points for a 50 $\mu$M PbS sample on the emission spectrum. The graphs are shifted vertically for clarity. (b) Similar effect for a 193 $\mu$M PbS sample. The inset compares the peak emission redshifts with distance for PbS and CdSe/ZnS samples.

Figure 3(a) is a comparison of the ratio of the short-circuit currents of the LSC ($I_{LSC}$) to that of the PV cell ($I_{PV}$) generated by the PbS and CdSe samples with QD concentration, measured using a broad band source simulating the solar spectrum. An interplay between absorption and SA results in a complicated variation in $I_{LSC}$ over the experimental range. At low concentrations, $I_{LSC}$ increases in both cases as more incident photons are absorbed. Then SA gradually offsets the enhanced absorption and slows this increase, leading to fewer photons reaching the PV cell at the edge. This slowdown begins around 3.2 $\mu$M for CdSe/ZnS and 70 $\mu$M for PbS samples. SA saturates at higher concentrations, which accounts for the eventual recovery of $I_{LSC}$, except that the high SA of CdSe/ZnS does not $I_{LSC}$ to recover completely. The smaller SA in PbS samples produce a different trend and $I_{LSC}$ picks up at high molarities with the 193 $\mu$M solution producing more than twice the maximum current of CdSe QDs. This current drops slightly after photoexposure.

Figure 3(b) compares $\eta_{opt}$ of PbS QDs to CdSe/ZnS QDs and Rhodamine B. While PbS demonstrates superior performance, it also exhibits a photoinstability that is inherent in these QDs.[15] There is a fast decay of the emission over a

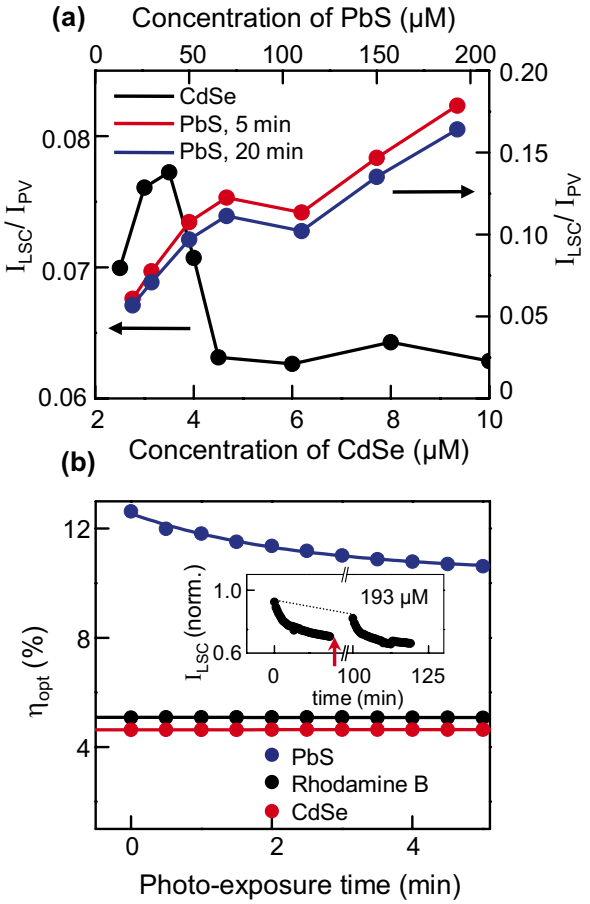


FIG. 3. (Color online) (a) LSC and PV current ratio as a function of QD solution concentration. Top and right axes correspond to PbS, bottom and left to CdSe/ZnS QDs. The response of PbS sample is shown at 5 and 20 min after illumination. (b) Integrated optical efficiency as a function of time for LSCs with different fluorescent species. Inset shows the reversal of photodarkening by blocking the incident radiation for a short period of time (arrow) in the PbS sample and the slower photo-oxidative decay (dotted line) by following the normalized $I_{LSC}$ over a few hours.

period of a few minutes that is known to be caused by photodarkening (or collective "blinking") and is reversible (seen in the inset). The rate of $I_{LSC}$ decay due to this effect is independent of the concentration of the QD solution, as is shown by the comparison of the two curves at 5 and 20 min in Fig. 3(a). In addition, there is also a slower, gradual, and permanent decay due to photo-oxidation, denoted by the dotted line in Fig. 3(b) (inset) which decreases $I_{LSC}$ at the rate of 0.1% per minute.

The efficiency is calculated as $\eta_{opt}=(I_{LSC}\times A_{PV}/I_{PV}\times A_{LSC})$, where $A_{LSC}$ the area of the top of the LSC and $A_{PV}$ the active area of the PV cell. The ratio $A_{LSC}/A_{PV}$ is known as the geometric factor, which is 11 in these samples. Along the short edge of the device the maximum $\eta_{opt}=0.5\%$ for CdSe/ZnS, typical for this material.[7] For PbS the highest single edge $\eta_{opt}$ measured is 1.4 %, and collection along all four edges leads to $\eta_{opt}=12.6\%$. This ninefold increase is a result of a constant $I_{LSC}/I_{PV}$ while the geometric factor is reduced, a consequence of the small size of our samples. To use the more commonly used metric, we calculate the PCE for our samples as the ratio of power supplied by the PV cells attached to the edges to the solar power absorbed by the LSC. The PbS sample has a PCE of 3.2%, comparable to that of QD based solar cells.[16] The CdSe/ZnS and Rhodamine B samples have PCE values of 1.2% and 1.3%, respectively.

Self absorption has been considered a critical limiting factor in achieving high efficiency LSCs.[12,17] Using the measured values of $\eta_{opt}$, $\eta_{abs}$, and $\eta_{QY}$ the losses incurred through SA are estimated by expressing $\eta_{opt}$ as a product of $\eta_{abs}\eta_{QY}(1-\eta_L)$. For the 3 $\mu$M CdSe/ZnS and 50 $\mu$M PbS, $\eta_{abs}=22\%$ and 40% across the solar spectrum, while $\eta_{QY}$ (from vendor) =50% and 30%, respectively, which leads to SA accounting for approximately a 35% loss in CdSe/ZnS and a 29% loss in the 50 $\mu$M PbS sample, confirming the conclusions of the redshift measurements that PbS has marginally lower reabsorption probability. In the 193 $\mu$M PbS, where $\eta_{opt}$ is nearly thrice that of CdSe, $\eta_{abs}=70\%$ and SA loss increases to 30%. From these measurements and calculations it is indicated that the difference in performance between the two types of QDs is only partially owed to differences in their SAs. The broadband absorption of solar radiation in PbS has a far greater impact on $\eta_{opt}$.

Our results demonstrate that the photocurrent of LSCs can be improved by using lower band gap QDs which are a better matched to the silicon solar cell. By designing NIR QDs with higher QY, and finding means of stabilizing their photoinduced instabilities,[18] the PCE of QD LSCs can be greatly enhanced.[19,20]

S.G. would like to acknowledge support from NSF Award No. DMR-0821771 and Shrink Nanotechnologies, Inc.

[1]W. H. Weber and J. Lambe, Appl. Opt. **15**, 2299 (1976).
[2]A. Goetzberger and W. Greubel, Appl. Phys. **14**, 123 (1977).
[3]A. F. Mansour, M. G. El-Shaarawy, S. M. El-Bashir, M. K. El-Mansy, and M. Hammam, Polym. Test. **21**, 277 (2002).
[4]A. F. Mansour, H. M. A. Killa, S. Abd El-Wanees, and M. Y. El-Sayed, Polym. Test. **24**, 519 (2005).
[5]K. Barnham, J. L. Marques, J. Hassard, and P. O'Brien, Appl. Phys. Lett. **76**, 1197 (2000).
[6]M. H. V. Werts, J. W. Hofstraat, F. A. J. Geurts, and J. W. Verhoeven, Chem. Phys. Lett. **276**, 196 (1997).
[7]V. Sholin, J. D. Olson, and S. A. Carter, J. Appl. Phys. **101**, 123114 (2007).
[8]A. J. Chatten, K. W. J. Barnham, B. F. Buxton, N. J. Ekins-Daukes, and M. A. Malik, Sol. Energy Mater. Sol. Cells **75**, 363 (2003).
[9]K. R. McIntosh, G. Lau, J. N. Cotsell, K. Hanton, D. L. Batzner, F. Bettiol, and B. S. Richards, Prog. Photovoltaics **17**, 191 (2009).
[10]W. Lü, I. Kamiya, M. Ichida, and H. Ando, Appl. Phys. Lett. **95**, 083102 (2009).
[11]W. A. Shurcliff and R. C. Jones, J. Opt. Soc. Am. **39**, 912 (1949).
[12]R. W. Olson, R. F. Loring, and M. D. Fayer, Appl. Opt. **20**, 2934 (1981).
[13]F. W. Wise, Acc. Chem. Res. **33**, 773 (2000).
[14]L. Bakueva, I. Gorelikov, S. Musikhin, X. S. Zhao, E. H. Sargent, and E. Kumacheva, Adv. Mater. (Weinheim, Ger.) **16**, 926 (2004).
[15]J. J. Peterson and T. D. Krauss, Phys. Chem. Chem. Phys. **8**, 3851 (2006).
[16]Y.-L. Lee and Y.-S. Lo, Adv. Funct. Mater. **19**, 604 (2009).
[17]M. J. Currie, J. K. Mapel, T. D. Heidel, S. Goffri, and M. A. Baldo, Science **321**, 226 (2008).
[18]G. I. Koleilat, L. Levina, H. Shukla, S. H. Myrskog, S. Hinds, A. G. Pattantyus-Abraham, and E. H. Sargent, ACS Nano **2**, 833 (2008).
[19]U. Rau, F. Einsele, and G. C. Glaeser, Appl. Phys. Lett. **87**, 171101 (2005).
[20]M. G. Hyldahl, S. T. Baileya, and B. P. Wittmershaus, Solar Energy **83**, 566 (2009).